

Meta-learning the mirror map in policy mirror descent

Carlo Alfano^{1,2}, Sebastian Towers^{3,4}, Silvia Sapora^{2,3,4}, Chris Lu⁴, and Patrick Rebeschini²

¹Email: carlo.alfano@stats.ox.ac.uk

²Department of Statistics, University of Oxford

³Equal contribution

⁴Department of Engineering, University of Oxford

Abstract

Policy Mirror Descent (PMD) is a popular framework in reinforcement learning, serving as a unifying perspective that encompasses numerous algorithms. These algorithms are derived through the selection of a mirror map and enjoy finite-time convergence guarantees. Despite its popularity, the exploration of PMD’s full potential is limited, with the majority of research focusing on a particular mirror map—namely, the negative entropy—which gives rise to the renowned Natural Policy Gradient (NPG) method. It remains uncertain from existing theoretical studies whether the choice of mirror map significantly influences PMD’s efficacy. In our work, we conduct empirical investigations to show that the conventional mirror map choice (NPG) often yields less-than-optimal outcomes across several standard benchmark environments. By applying a meta-learning approach, we identify more efficient mirror maps that enhance performance, both on average and in terms of best performance achieved along the training trajectory. We analyze the characteristics of these learned mirror maps and reveal shared traits among certain settings. Our results suggest that mirror maps have the potential to be adaptable across various environments, raising questions about how to best match a mirror map to an environment’s structure and characteristics.

1 Introduction

Policy gradient (PG) methods (Williams & Peng, 1991; Sutton et al., 1999; Konda & Tsitsiklis, 2000; Baxter & Bartlett, 2001) are some of the most widely-used mechanisms for policy optimization in reinforcement learning (RL). These algorithms are gradient-based methods that optimize over a class of parameterized policies and have become a popular choice for RL problems, both in theory (Kakade, 2002; Peters & Schaal, 2008; Bhatnagar et al., 2009; Schulman et al., 2015; Mnih et al., 2016; Schulman et al., 2017; Lan, 2022a) and in practice Shalev-Shwartz et al. (2016); Berner et al. (2019); Ouyang et al. (2022).

Among PG methods, some of the most successful algorithms are those that employ some form of regularization in their updates, ensuring that the newly updated policy retains some degree of similarity to its predecessor. This principle has been implemented in different ways. For instance, trust region policy optimization (TRPO) Schulman et al. (2015) imposes a Kullback-Leibler divergence Kullback & Leibler (1951) hard constraint for its updates, while proximal policy optimization (PPO) (Schulman et al., 2017) uses a clipped objective to penalize large updates. A framework that has recently attracted attention and belongs to this heuristic is that of policy mirror descent (PMD) (Tomar et al., 2022; Lan, 2022a; Xiao, 2022; Kuba et al., 2022; Vaswani et al., 2022; Alfano et al., 2023), which applies mirror descent Nemirovski & Yudin (1983) to RL to regularize the policy updates.

PMD consists of a wide class of algorithms, each derived by selecting a *mirror map* that introduces distinct regularization characteristics. In recent years, PMD has been investigated through numerical experiments (Tomar et al., 2022), but it has mainly been analysed from a theoretical perspective. To the best of our knowledge, research has been mostly focused either on the particular case of the negative entropy mirror map, which generates the natural policy gradient (NPG) algorithm (Kakade, 2002; Agarwal et al., 2021), or on finding theoretical guarantees for a generic mirror map.

NPG has been proven to converge to the optimal policy, up to a difference in expected return (or *error floor*), in several settings, e.g. using tabular, linear, or general parameterization (Agarwal et al., 2021) or regularizing rewards (Cen et al., 2021). It has been shown that NPG benefits from implicit regularization (Hu et al., 2022),

that it can exploit optimism (Zanette et al., 2021; Liu et al., 2023) and the empirical performance of some of its variants has been evaluated in several environments (Vaswani et al., 2022, 2023). When considering other specific mirror maps investigated in the RL literature, the Tsallis entropy has been noted for enhancing performance in offline settings (Tomar et al., 2022) and for offering improved sample efficiency in online settings (Li & Lan, 2023), when compared to the negative entropy.

There is a substantial body of theoretical research focused on the general case of mirror maps. This research demonstrates that PMD achieves convergence to the optimal policy under the same conditions as NPG, as evidenced by various studies (Xiao, 2022; Lan, 2022b; Yuan et al., 2023; Alfano et al., 2023). Except for the precise scenario in tabular settings, convergence guarantees are subject to an error floor due to the inherent randomness or bias within the algorithm. In the majority of PMD analyses involving generic mirror maps, both the convergence rate and the error floor show mild dependence on the specific choice of mirror map. Typically, the effect of the mirror map appears explicitly as a multiplicative factor in the convergence rate and it appears implicitly in the error floor. These analyses often rely on *upper bounds*, meaning they may not accurately reflect the algorithms’ actual performance in practical applications.

In this work, we contribute to the literature with an empirical investigation of PMD, in the setting of policies parameterized by neural networks. Firstly, we show that in most environments it is possible to learn a mirror map that performs significantly better than the negative entropy (NPG). Secondly, we demonstrate that the mirror map can significantly influence the error floor associated with PMD. In particular, we show that in several environments the best performance achieved by PMD with the negative entropy is much lower than the one achieved by the mirror map of our choice. Thirdly, we detail the mirror maps learned through our approach, highlighting how certain maps induce similar characteristics in the algorithm’s trajectory. Lastly, we pose and investigate the question of transferability, illustrating that a mirror map optimized for one environment can also yield effective results in another. To establish our findings, we employ approximate mirror policy optimization (AMPO) Alfano et al. (2023) as PMD framework, and we use evolution strategies (ES) to search for the mirror map that maximizes the performance of AMPO over an environment.

AMPO (Alfano et al., 2023) is a recently-proposed PMD framework that is designed to integrate general parameterization schemes, in our case neural networks, and arbitrary mirror maps. It benefits from theoretical guarantees, as Alfano et al. (2023) show that AMPO has quasi-monotonic updates as well as sub-linear and linear convergence rates, depending on the step-size schedule. These desirable properties make AMPO particularly suitable for our numerical investigation. In order to allow optimization over the space of mirror maps used by AMPO, we introduce a parameterization scheme for mirror maps. Specifically, we give a parameterization for ω -potentials, which have been shown to induce a class of mirror maps for which AMPO is computationally efficient (Krichene et al., 2015; Alfano et al., 2023).

ES are a type of population-based stochastic optimization algorithm that leverages random noise to generate a diverse pool of candidate solutions, and have been successfully applied to a variety of tasks (Real et al., 2019; Salimans et al., 2017; Such et al., 2018). The main idea consists in iteratively selecting higher-performing individuals, w.r.t. a fitness function, resulting in a gradual convergence towards the optimal solution. ES algorithms are gradient-free and have been shown to be well-suited for (meta-)optimisation problems where the objective function is noisy or non-differentiable and the search space is large or complex (Beyer, 2000; Lu et al., 2022, 2023). We use ES to search over the parameterized class of mirror maps we introduce, by defining the fitness of a particular mirror map as the average return across all training steps of AMPO, for a fixed environment and for given hyper-parameters of AMPO.

The rest of the paper is organized as follows. In Section 2, we introduce the setting of RL and explain in more detail the mirror descent algorithm. We summarise the results on AMPO by Alfano et al. (2023) and analyse the effect that mirror maps have on AMPO in Section 3. In Section 4, we describe the methodology behind our numerical experiments, which are then discussed in Section 5. Finally, we give our conclusions in Section 6.

2 Preliminaries

2.1 Reinforcement Learning

Define a discounted Markov Decision Process (MDP) as the tuple $\mathcal{M} = (\mathcal{S}, \mathcal{A}, P, r, \gamma, \mu)$, where \mathcal{S} and \mathcal{A} are respectively the state and action spaces, $P(s' | s, a)$ is the transition probability from state s to s' when taking action a , $r(s, a) \in [0, 1]$ is the reward function, γ is a discount factor, and μ is a starting state distribution. A

policy $\pi \in (\Delta(\mathcal{A}))^{\mathcal{S}}$, where $\Delta(\mathcal{A})$ is the probability simplex over \mathcal{A} , represents the behavior of an agent on an MDP, whereby at state $s \in \mathcal{S}$ the agents takes actions according to the probability distribution $\pi(\cdot | s)$. Our objective is for the agent to find a policy that maximizes the expected discounted cumulative reward for the starting state distribution μ . That is, we want to find

$$\pi^* \in \operatorname{argmax}_{\pi \in (\Delta(\mathcal{A}))^{\mathcal{S}}} \mathbb{E}_{s \sim \mu} [V^\pi(s)]. \quad (1)$$

Here $V^\pi : \mathcal{S} \rightarrow \mathbb{R}$ denotes the *value function* associated with policy π and is defined as

$$V^\pi(s) := \mathbb{E} \left[\sum_{t=0}^{\infty} \gamma^t r(s_t, a_t) \mid \pi, s_0 = s \right],$$

where s_t and a_t are the current state and action at time t and the expectation is taken over the trajectories generated by $a_t \sim \pi(\cdot | s_t)$ and $s_{t+1} \sim P(\cdot | s_t, a_t)$. Similarly to the value function, we define the Q-function associated with a policy π as

$$Q^\pi(s, a) := \mathbb{E} \left[\sum_{t=0}^{\infty} \gamma^t r(s_t, a_t) \mid \pi, s_0 = s, a_0 = a \right],$$

where the expectation is once again taken over the trajectories generated by the policy π . We also define the discounted state visitation distribution as

$$d_\mu^\pi(s) := (1 - \gamma) \mathbb{E}_{s_0 \sim \mu} \left[\sum_{t=0}^{\infty} \gamma^t P(s_t = s \mid \pi, s_0) \right],$$

where $P(s_t = s \mid \pi, s_0)$ represents the probability of the agent being in state s at time t when following policy π and starting from s_0 . The probability distribution over states $d_\mu^\pi(s)$ represents the stationary distribution induced by π .

2.2 Mirror descent

We review the mirror descent (MD) framework, starting from mirror maps Bubeck (2015). Let $\mathcal{X} \subseteq \mathbb{R}^A$ be a convex set. A *mirror map* $h : \mathcal{X} \rightarrow \mathbb{R}$ is a strictly convex, continuously differentiable and essentially smooth function¹ that satisfies $\nabla h(\mathcal{X}) = \mathbb{R}^A$. The convex conjugate of h is defined as

$$h^*(x^*) := \sup_{x \in \mathcal{X}} \langle x^*, x \rangle - h(x), \quad x^* \in \mathbb{R}^A.$$

The mirror map h and its convex conjugate h^* enable us to map objects from the primal space \mathcal{X} to its dual space \mathbb{R}^A , $x \mapsto \nabla h(x)$, and conversely, $x^* \mapsto \nabla h^*(x^*)$. Specifically, we have that, for all $(x, x^*) \in \mathcal{Y} \times \mathbb{R}^A$,

$$x = \nabla h^*(\nabla h(x)) \quad \text{and} \quad x^* = \nabla h(\nabla h^*(x^*)). \quad (2)$$

The *Bregman divergence* Bregman (1967); Censor & Zenios (1997) induced by the mirror map h is defined as

$$\mathcal{D}_h(x, y) := h(x) - h(y) - \langle \nabla h(y), x - y \rangle,$$

where $\mathcal{D}_h(x, y) \geq 0$ for all $x, y \in \mathcal{Y}$. Given a convex optimization problem $\min_{x \in \mathcal{C}} V(x)$, where $\mathcal{C} \subseteq \mathcal{X}$ is a convex set and $V : \mathcal{C} \rightarrow \mathbb{R}$ is a differentiable function, the MD algorithm Nemirovski & Yudin (1983); Bubeck (2015) can be used to solve it. It can be formalized as a two-step iterative algorithm: for all $t \geq 0$,

$$y^{t+1} = \nabla h(x^t) - \eta_t \nabla V(x)|_{x=x^t}, \quad (3)$$

$$x^{t+1} = \operatorname{Proj}_{\mathcal{X}}^h(\nabla h^*(y^{t+1})), \quad (4)$$

where η_t follows a step-size schedule $(\eta_t)_{t \geq 0}$ and $\operatorname{Proj}_{\mathcal{X}}^h(\cdot)$ is the *Bregman projection*

$$\operatorname{Proj}_{\mathcal{X}}^h(y) := \operatorname{argmin}_{x \in \mathcal{X}} \mathcal{D}_h(x, y). \quad (5)$$

¹A function h is *essentially smooth* if $\lim_{x \rightarrow \partial \mathcal{X}} \|\nabla h(x)\|_2 = +\infty$, where $\partial \mathcal{X}$ denotes the boundary of \mathcal{X} .

Algorithm 1 Approximate Mirror Policy Optimization

Input: Initial policy π^0 , mirror map h , parameterization class \mathcal{F}^Θ , iteration number T , step-size schedule $(\eta_t)_{t \geq 0}$, state-action distribution sequence $(v^t)_{t \geq 0}$.

for $t = 0$ **to** $T - 1$ **do**

1) Obtain $\theta^{t+1} \in \Theta$ such that

$$\theta^{t+1} \in \operatorname{argmin}_{\theta \in \Theta} \|f^\theta - Q^t - \eta_t^{-1} \nabla h(\pi^t)\|_{L_2(v^t)}^2.$$

2) Update

$$\pi_s^{t+1} = \operatorname{Proj}_{\Delta(\mathcal{A})}^h(\nabla h^*(\eta_t f_s^{t+1})), \quad \forall s \in \mathcal{S}.$$

end for

3 Approximate Mirror Policy Optimization

The algorithmic framework we consider for our simulations is Approximate Mirror Policy Optimization (AMPO) Alfano et al. (2023), which is described in Algorithm 1. We give here a brief description of the algorithm and a summary of its theoretical guarantees. For ease of exposition, we define the following shorthand: for each iteration t of Algorithm 1, let $\pi^t := \pi^{\theta^t}$, $V^t := V^{\pi^t}$, $Q^t := Q^{\pi^t}$, $f^t := f^{\theta^t}$, and $d_\mu^t := d_\mu^{\pi^t}$. For any function $y : \mathcal{S} \times \mathcal{A} \rightarrow \mathbb{R}$ and distribution v over $\mathcal{S} \times \mathcal{A}$, let $y_s := y(s, \cdot) \in \mathbb{R}^{\mathcal{A}}$ and $\|y\|_{L_2(v)}^2 = \mathbb{E}_{(s,a) \sim v}[y(s,a)^2]$. Given a parameterized function class $\mathcal{F}^\Theta = \{f^\theta : \mathcal{S} \rightarrow \mathbb{R}^{\mathcal{A}}, \theta \in \Theta\}$, AMPO consists in a two-step iterative update based on the mirror descent algorithm described in (3) and (4), where the dual iterate y^t is replaced by the scoring function f^t and the gradient of the objective function is replaced by Q^t . At each iteration t , step 1) in Algorithm 1 is an approximation of (3), where we want f^{t+1} to be close to $Q^t + \eta_t^{-1} \nabla h(\pi^t)$ in L_2 -norm, w.r.t. an arbitrary distribution v^t . The updated policy is then obtained in step 2) by projecting the scoring function onto the probability simplex, using a Bregman projection. AMPO benefits from theoretical guarantees, provided the following assumptions are satisfied.

(A1) (*Approximation error*). There exists $\varepsilon_{\text{approx}} \geq 0$ such that, for all times $t \geq 0$,

$$\mathbb{E}[\|f^{t+1} - Q^t - \eta_t^{-1} \nabla h(\pi^t)\|_{L_2(v^t)}^2] \leq \varepsilon_{\text{approx}},$$

where $(v^t)_{t \geq 0}$ is a sequence of distributions over states and actions and the expectation is taken over the randomness of AMPO.

(A2) (*Concentrability coefficient*). There exists $C_v \geq 0$ such that, for all times t ,

$$\mathbb{E}_{(s,a) \sim v^t} \left[\left(\frac{d_\mu^\pi(s) \pi(a | s)}{v^t(s, a)} \right)^2 \right] \leq C_v,$$

whenever (d_μ^π, π) is either (d_μ^*, π^*) , (d_μ^{t+1}, π^{t+1}) , (d_μ^*, π^t) , or (d_μ^{t+1}, π^t) .

(A3) (*Distribution mismatch coefficient*). Let $d_\mu^* := d_\mu^{\pi^*}$. There exists $\nu_\mu \geq 0$ such that

$$\max_{s \in \mathcal{S}} \frac{d_\mu^*(s)}{d_\mu^t(s)} \leq \nu_\mu, \quad \text{for all times } t \geq 0.$$

Theorem 3.1. (Alfano et al., 2023, Theorem 4.3). *Let (A1), (A2) and (A3) be true. If the step-size schedule is non-decreasing, i.e., $\eta_t \leq \eta_{t+1}$ for all $t \geq 0$, the iterates of Algorithm 1 satisfy: for every $T \geq 0$,*

$$V^*(\mu) - \frac{1}{T} \sum_{t < T} \mathbb{E}[V^t(\mu)] \leq \underbrace{\frac{1}{T} \left(\frac{\mathcal{D}_0^*}{(1-\gamma)\eta_0} + \frac{\nu_\mu}{1-\gamma} \right)}_{\text{convergence rate}} + \underbrace{\frac{2(1+\nu_\mu)\sqrt{C_v \varepsilon_{\text{approx}}}}{1-\gamma}}_{\text{error floor}},$$

where $\mathcal{D}_0^* = \mathbb{E}_{s \sim d_\mu^*}[\mathcal{D}_h(\pi_s^*, \pi_s^0)]$.

While Theorem 3.1 improves upon previous results by relaxing the conditions for $\mathcal{O}(1/T)$ convergence of PMD with general function approximation, its statement is similar to many results in the literature on PMD and NPG (Agarwal et al., 2021; Xiao, 2022; Lan, 2022b; Hu et al., 2022). That is, the convergence guarantee involves two terms, i.e. a convergence rate, which involves the Bregman divergence between the optimal policy and the starting policy, and an error floor, which involves the approximation error. Given that by setting $\eta_0 = \mathcal{D}_0^*/\nu_\mu$ we obtain the convergence rate $2\nu_\mu(T(1-\gamma))^{-1}$, and that the error floor has no explicit dependence on the mirror map, Theorem 3.1 suggests that the mirror map has a mild influence on the performance of AMPO. The only way the mirror map and the step-size seem to affect the convergence guarantee is, implicitly, by changing the path of the algorithm and therefore influencing the parameters in Assumptions (A1), (A2), and (A3). Similar observations can be made from several results in the PMD literature that share the same structure of convergence guarantees. One of the contributions of our work is to challenge and refute these conclusions, highlighting a gap between theoretical guarantees, which are *based on upper bounds*, and the actual performance observed in PMD-based methodologies. Our empirical studies reveal that the choice of mirror map and step-size significantly influence both the speed of convergence and the minimum achievable error floor in AMPO.

3.1 ω -potential mirror maps

As already highlighted by Alfano et al. (2023), mirror maps that are induced by ω -potentials allow to compute the Bregman projection in step 2) of Algorithm 1 with $\tilde{\mathcal{O}}(|\mathcal{A}|)$ operations and simplify the minimization problem in step 1). Here, the notation $\tilde{\mathcal{O}}(\cdot)$ hides logarithmic terms. Given this desirable property, we restrict our study to this class of mirror maps. We give here a short summary on how to use ω -potentials for AMPO and discuss the effects that different potentials have on the training path. Here and in the rest of the paper, we set the step-size schedule $(\eta_t)_{t \geq 0}$ equal to a constant value η .

Definition 3.2 (ω -potential mirror map Krichene et al. (2015)). For $u \in (-\infty, +\infty]$, $\omega \leq 0$, an ω -potential is defined as an increasing C^1 -diffeomorphism $\phi : (-\infty, u) \rightarrow (\omega, +\infty)$ such that

$$\lim_{x \rightarrow -\infty} \phi(x) = \omega, \quad \lim_{x \rightarrow u} \phi(x) = +\infty, \quad \int_0^1 \phi^{-1}(x) dx \leq \infty.$$

For any ω -potential ϕ , we define the associated mirror map h_ϕ as

$$h_\phi(\pi_s) = \sum_{a \in \mathcal{A}} \int_1^{\pi(a|s)} \phi^{-1}(x) dx.$$

Krichene et al. (2015, Proposition 2) prove that, in the setting of ω -potential mirror maps, the Bregman projection in step 2) of Algorithm 1 can be performed using a bisection algorithm with $\tilde{\mathcal{O}}(|\mathcal{A}|)$ computations. The updated policy π^{t+1} can be expressed, for all $s \in \mathcal{S}, a \in \mathcal{A}$, as

$$\pi^{t+1}(a | s) = \sigma(\phi(\eta f^{t+1}(s, a) + \lambda_s^{t+1})), \quad (6)$$

where $\lambda_s^{t+1} \in \mathbb{R}$ is a normalization factor to ensure $\pi_s^{t+1} \in \Delta(\mathcal{A})$ for all $s \in \mathcal{S}$, and $\sigma(z) = \max(z, 0)$ for $z \in \mathbb{R}$. Additionally, we can rewrite the minimization problem in step 1) of Algorithm 1 as

$$\theta^{t+1} \in \operatorname{argmin}_{\theta \in \Theta} \|f^\theta - Q^t - \eta^{-1} \max(\eta f^t + \lambda_s^t, \phi^{-1}(0))\|_{L_2(v^t)}^2, \quad (7)$$

where $\max(\cdot, \cdot)$ is applied element-wisely, and we used (6) and the definition of the ω -potential mirror map h_ϕ . Assuming for simplicity that $\phi(x) > 0$ for all $x \in \mathbb{R}$, the minimization problem in (7) implies that, at each iteration t , f^t is an approximation of the sum of the Q-functions up to that point, that is $f^t \simeq \sum_{i=0}^{t-1} Q^i$. Therefore, the scoring function f^t serves as an estimator of the value of an action.

When $\phi(x) = e^x$ we recover the negative entropy mirror map (see Appendix A.1), which is the standard choice of mirror map in the RL literature (Agarwal et al., 2021; Tomar et al., 2022; Hu et al., 2022; Vaswani et al., 2022, 2023). One of the primary objectives of this work is to motivate further research into the choice of mirror maps, as influenced by the choice of the function ϕ , moving beyond the conventional use of $\phi(x) = e^x$. This is achieved by examining how different choices of ϕ influence the trajectory of training and demonstrating that, in many cases, there is a mirror map that outperforms the negative entropy by a large margin.

We start by illustrating two properties of ω -potentials in the context of AMPO.

Proposition 3.3. *Let η, η' be two step-sizes, and ϕ, ϕ' be two ω -potentials. We say that (η, ϕ) and (η', ϕ') are equivalent for AMPO if they generate the same training path.*

We have that:

- (shift-invariant) if $\phi'(x) := \phi(x + c)$, for $c \in \mathbb{R}$, and $\eta = \eta'$, then (η, ϕ) and (η', ϕ') are equivalent for AMPO;
- (scale-invariant) if $(\eta', \phi'(x)) = (c\eta, \phi(x/c))$, for $c \in \mathbb{R}$, then (η, ϕ) and (η', ϕ') are equivalent for AMPO.

We refer to Appendix A.2 for a proof. The shape of the ω -potential ϕ determines how the scores obtained by multiplying the scoring function f^θ and the step-size η are transformed into probabilities, as shown in (6). As an example, when $\phi(x) = e^x$, the scores are transformed into probabilities through a softmax operator. In Figure 1 we show different possible ω -potentials, together with the probabilities that they induce in the two action case for different scores, using (6). Since ϕ is shift invariant, the induced distribution depends only on the difference between the scores the two actions are assigned, i.e. $|\eta f^\theta(s, a_1) - \eta f^\theta(s, a_2)|$, for an arbitrary state s . For the same scores, very different distributions are induced. For example, the *double sigmoid* ϕ induces a distribution with higher entropy, or more *exploratory*, for small score differences w.r.t. the other ω -potentials. On the other hand, it induces a lower entropy distribution, or *greedier*, for high score differences w.r.t. the other ω -potentials. Given that the scores reflect an estimate of the value of the actions, a smaller score difference implies higher uncertainty in the ranking of the values of the actions. Therefore, we call a policy *greedier* than another because it assigns more probability to the top scored action, for the same score differences or level of uncertainty. On the other hand, we call a policy more *exploratory* than another because it assigns more probability to actions other than the top ranked one for the same score differences, continuing to explore the environment.

Remark 3.4. In the setting of AMPO, we can describe how a score update is reflected on the updated policy. Assume that $\mathcal{A} = \{a_1, a_2\}$ and, for an arbitrary state s and iteration t , let $b, c \in \mathbb{R}$ such that $\eta f^{t+1}(s, a_1) = \eta f^t(s, a_1) + b + c$ and $\eta f^{t+1}(s, a_2) = \eta f^t(s, a_2) + b$. In this setting, where the score difference between the two actions has increased (or diminished) by a factor c , we have that the derivative of the updated policy w.r.t. c is

$$\frac{d\pi^{t+1}(a_1|s)}{dc} = \frac{\phi'(x_1)\phi'(x_2)}{\phi'(x_1) + \phi'(x_2)}, \quad (8)$$

$$\frac{d\pi^{t+1}(a_2|s)}{dc} = -\frac{\phi'(x_1)\phi'(x_2)}{\phi'(x_1) + \phi'(x_2)}, \quad (9)$$

where $x_i = \eta f^{t+1}(s, a_i) + \lambda_s^{t+1}$. The two terms in (8) and (9) describe by how much the updated policy changes for an infinitesimal change of c , depending on ϕ . We provide more details and a proof in Appendix A.2.

Figure 1 and Remark 3.4 show that the choice of the ω -potential ϕ can influence greatly how AMPO transforms scores into policies, and, therefore, how it tackles the exploration/exploitation trade-off. We refer to Appendix A.4 for further discussion on the case with multiple actions.

4 Methodology

We give a description of the methodology behind our empirical investigation of PMD. We first introduce the parameterization class we have chosen for the ω -potential ϕ and follow by explaining the meta-learning procedure that we run over it in order to maximize the average return of AMPO.

4.1 Parameterization for ϕ

We define a finite dimensional subspace of the ω -potential mirror map class with an accompanying parameterization, to computationally search over it. The properties in Proposition 3.3 mean that for each pair (η, ϕ) , there are infinitely-many equivalent pairs of step-size and ω -potential, which is undesirable in practice. To simplify the meta-optimization problem, we require that the parameterized class must not exhibit shift invariance or scale invariance.

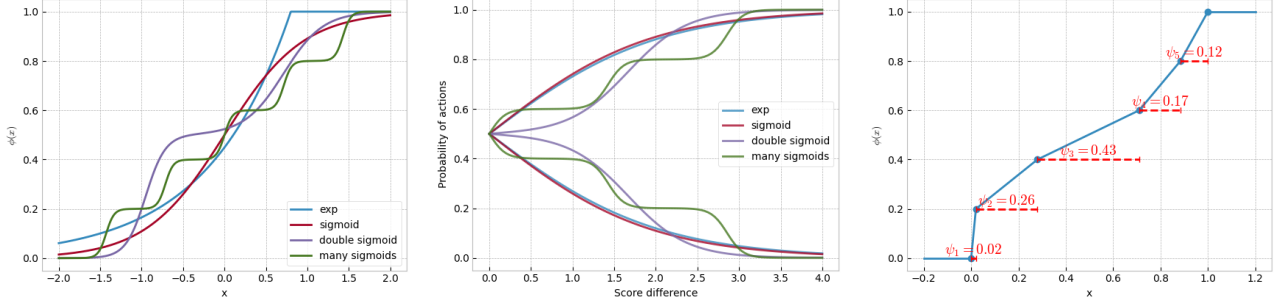


Figure 1: **(Left and Center)** Examples for ϕ , and the resulting effect on the policy. We show only the two action case, to the “Score difference” refers to the difference between the two actions (for a given state). “exp” refers to the exponential function. “sigmoid” is the logistic function ($x \mapsto (1 + e^{-x})^{-1}$). “double sigmoid” is the average of two offset logistic functions, and “many sigmoids” is the average of five offset logistic functions. The exact functions can be found in Appendix A.3. **(Right)** A plot visually demonstrating the parameterization we use, whereby each segment traverses a fixed vertical displacement

Let Δ_n be the n -dimensional probability simplex. We define the parameterized class $\Phi = \{\phi_\psi : \mathbb{R} \rightarrow [0, 1], \psi \in \Delta_n\}$, with

$$\phi_\psi(x) = \begin{cases} 0 & \text{if } x \leq 0, \\ \frac{x}{\psi_1 n} & \text{if } 0 < x \leq \psi_1, \\ \frac{j}{n} + \frac{x - \sum_{i=1}^j \psi_i}{n\psi_{j+1}} & \text{if } \sum_{i=1}^j \psi_i < x \leq \sum_{i=1}^{j+1} \psi_i, \\ 1 & \text{if } x > 1, \end{cases}$$

where $1 \leq j \leq n - 1$. In other words, ϕ is defined as a piece-wise linear function with n steps where, for all $j \leq n$, $\phi(\sum_{i=1}^j \psi_i) = j/n$ and subsequent points are interpolated with a straight segment. This is illustrated in Figure 1. In practice, we enforce $\psi \in \Delta_n$ by normalizing the parameters outputted by the ES algorithm. That is, for a parameter vector $y \in \mathbb{R}^n$, we apply the transformation $\psi_i = |y_i| / \sum_{j=1}^n |y_j|$, for all $i = 1, \dots, n$. We have that ω -potentials within Φ are not shift-invariant or scale-invariant, since we enforce $\phi_\psi(0) = 0$ and $\phi_\psi(1) = 1$.

We note that the ω -potentials within Φ violate some of the constraints in Definition 3.2, as they are non-decreasing instead of increasing and $\lim_{x \rightarrow \infty} \phi(x) = 1$ for all $\phi \in \Phi$. In Appendix A.5, we show that, if $\phi \in \Phi$, we can construct an ω -potential ϕ' that satisfies the constraints in Definition 3.2 such that ϕ and ϕ' induce the same computations and policies along the path of AMPO.

4.2 Meta-learning

Our aim is to find meta-parameters ψ for ϕ that maximise the average return over the training of our agent. That is, we want to find

$$\psi^* \in \operatorname{argmax}_{\psi \in \Psi} \left[\frac{1}{T} \sum_{t < T} \mathbb{E} [V^t(\mu)] \right],$$

where the expectation is taken over the randomness of AMPO and the policies π^1, \dots, π^{T-1} are induced by ϕ_{ψ^*} .

To effectively meta-learn the hyperparameters, we employ the Separable Covariance Matrix Adaptation Evolution Strategy (sep-CMA) (Ros & Hansen, 2008), a variant of the popular algorithm CMA-ES (Hansen & Ostermeier, 2001). CMA-ES is, essentially, a second-order method adapted for gradient free optimization. At every generation, it samples n new points from a normal distribution, parameterized by a mean vector m_k and a covariance matrix C_k . That is, the samples for generation k , x_1^k, \dots, x_n^k , are distributed i.i.d. according to $x_i^k \sim \mathcal{N}(m_k, C_k)$. For each generation k , denote the $m \leq n$ best performing samples as $x_1^{*k} \dots x_m^{*k}$. Then update the mean vector as $m_{k+1} = \sum_{i=1}^m w_i x_i^{*k}$, where $\sum_{i=1}^m w_i = 1$, so that the next generation is distributed around the weighted mean of the best performing samples. C_{k+1} is also updated to reflect the covariance structure of $x_1^{*k} \dots x_m^{*k}$, in a complex way beyond the scope of this text.

Due to the need to update C_k based on covariance information, CMA-ES exhibits a quadratic scaling behavior with respect to the dimensionality of the search space, potentially hindering its efficiency in high-dimensional settings. To improve computational efficiency, we adopt sep-CMA, which introduces a diagonal constraint on the covariance matrix and reduces the computational complexity of the algorithm.

5 Experiments

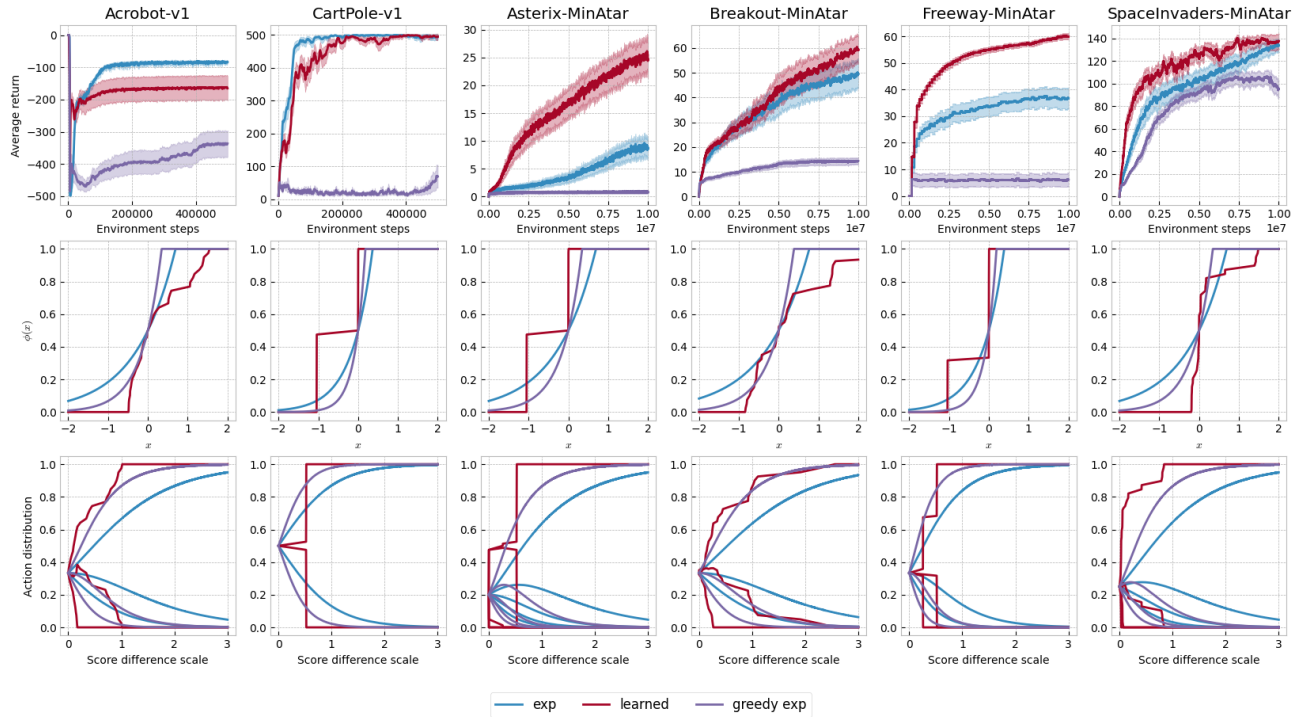


Figure 2: Comparison between the meta-learned potential ϕ and the potentials exp and greedy-exp across a range of standard environments. The top plots display a shaded region denoting the standard error around the mean lines (averaged over 20 realizations). In the middle plots, we utilize the potential’s shift-invariance property by setting $\phi(0) = 0.5$, enabling a direct comparison between the potentials.

In this section, we discuss the results of our numerical experiments. In Section 5.1, we describe the experimental setup. In Section 5.2, we show the performance of AMPO with the learned mirror map against the negative entropy for a variety of environments. We comment on the learned mirror maps in Section 5.3 and we show how a mirror map learned on one environment performs on others in Section 5.4.

5.1 Experimental setup

Model architecture and training We optimize the hyper-parameters of AMPO for the negative entropy mirror map for each environment, using the hyper-parameter tuning framework Optuna (Akiba et al., 2019). This is done to ensure we are looking at a fair benchmark of performance using the negative entropy mirror map. We report the chosen hyper-parameters in Appendix B.1. We then initialize (η, ϕ_ψ) so that they are close to being equivalent to $(1, e^x)$ for AMPO². We then run Sep-CMA-ES on each environment separately. The whole training procedure is implemented in JAX, using gymnasium environments (Lange, 2022b) and evosax (Lange, 2022a) for the evolution. We run on 8 GTX 1080Ti GPUs, and the optimization process takes roughly 48 hours for a single environment. Details are given in Appendix B. We will open source the code for our simulations upon a camera-ready release of this work.

²We achieve this by assigning $\psi_i \propto \log(i/(i-1))$, for $i = 2, \dots, n$, and setting $\psi_1 \propto 3 \log(10)$.

Environments We test AMPO on the Basic Control Suite (BCS) and the MinAtar Suite. For BCS, we run the evolution for 600 generation, each with 500k timesteps. For MinAtar, we run the evolution for 500 generation with 1M timesteps, then run 100 more generations with 10M timesteps.

5.2 Benchmark evaluation

Our empirical results are illustrated in Figure 2, where we compare the performance of AMPO with the meta-learned ω -potential against AMPO with the optimally-tuned negative entropy mirror map $\phi(x) = e^x$. Additionally, we show the performance for $\phi(x) = e^{2x}$, which is equivalent to doubling η for the negative entropy and induces greedier policies for the same action scores. For all environments and mirror maps, we use the hyper-parameters returned by Optuna for AMPO with the negative entropy. We refer to the meta-learned ω -potential as *learned- ϕ* , to the exponential potential as *exp- ϕ* , and to $\phi(x) = e^{2x}$ as *greedy-exp- ϕ* .

Across the six environments tested, our learned- ϕ leads to a better overall performance in the MinAtar environments, to a similar performance in CartPole-v1, and to a worse performance in Acrobot-v1. We observe the largest improvement in performance on Asterix and Freeway, where the average return for learned- ϕ is, respectively, more than double and almost double the one for exp- ϕ . In Breakout and SpaceInvaders, we observe that the curve for the average return associated to learned- ϕ dominates that one associated to exp- ϕ . We observe that the performance in CartPole is similar for the two mirror maps and that the performance associated to learned- ϕ does not match the one associated to exp- ϕ in Acrobot. As to greedy-exp- ϕ , Figure 2 shows that its performance is remarkably worse than the one for exp- ϕ across all environments, which demonstrates that both the shape of ϕ and the step-size play a role in the performance of AMPO. Additionally, while both learned- ϕ and greedy-exp- ϕ assign a higher probability than exp- ϕ to the top ranking action in most environments, Figure 2 shows that this property is not sufficient to achieve better performance.

Figure 2 also shows that different mirror maps may result in different error floors. In Acrobot we have that the performance for exp- ϕ converges to a higher average return than the one for learned- ϕ , while the opposite happens in Freeway and in Asterix, although the algorithm does not seem to have fully converged in the latter. Moreover, we have that the performance associated to greedy-exp- ϕ converges to a much lower level across all environments.

5.3 Learned mirror maps

The meta-learned ω -potentials exhibit shared properties, which can be seen from Figure 2. The first shared property is that all learned- ϕ assign 0 probability to the worst actions for relatively small score difference scales, whilst exp- ϕ always assigns some weight. In more complex environments, where the evaluation of a certain action maybe be strongly affected by noise or where the optimal state may be combination locked Misra et al. (2020), this behaviour may lead to a critical lack of exploration. However, it appears that this is not the case in these environment, and we hypothesise that by setting the probability of the worst actions to 0 the learned ω -potentials avoid wasting samples and hence can converge to the optimal policy more rapidly.

The second shared property, among the learned- ϕ for Cartpole-v1, Asterix-MinAtar, and Freeway-Minatar, is assigning similar probabilities to the best actions for small score difference scales. In CartPole and Asterix, the associated learned- ϕ induces almost all of the probability mass to be placed on the two best actions, when the scores are close enough. Once the scores are sufficiently apart, the associated learned- ϕ induces a greedy policy, which only selects the highest-scoring action. Freeway shows a similar behaviour. The associated learned- ϕ induces the policy to be uniform on the top three actions initially, before switching to splitting the probability mass between the top two, and finally being completely greedy, for an increasing score difference scale. We believe that this behaviour can be justified by the concept of *effective horizon* introduced by Laidlaw et al. (2023), whereby in environments with a short effective horizon the Q-functions associated with the optimal and uniform policy rank the actions in a similar manner. The learned learned- ϕ seems to be exploiting this property of the environments, by initially exploring the state and action spaces and switching to a deterministic policy once the agent has obtained a precise enough ranking of the actions.

5.4 Transferability of mirror maps

For each learned- ϕ , Figure 3 shows the averaged performance of the associated AMPO instance across all environments, demonstrating whether a mirror map is able to transfer what it learned from one environment to another. We see strong transferability among CartPole, Asterix, and Freeway, these three environments being the ones where

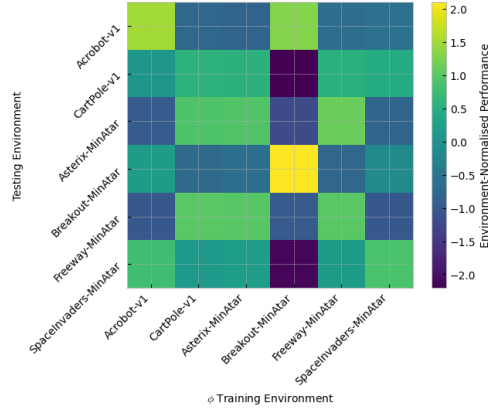


Figure 3: Transferability of ϕ across environments. For each testing environment, performances are normalised by the mean and standard deviation. Raw values may be found in the appendix.

the learned- ϕ induces an algorithm which will rapidly switch the policy from random to selecting deterministically the best ranked action. Figure 3 also shows that learned- ϕ from Breakout is the only one that presents significantly weak transferability across most environments, performing poorly on both SpaceInvaders and CartPole.

6 Conclusion

Our study presents an empirical examination of PMD properties, outlining a gap between theoretical findings established in the literature and the actual performance of PMD methods on benchmarks. Leveraging the PMD framework from AMPO along with the ES meta-learning method, we successfully trained mirror maps that largely outperform negative entropy in various environments. These optimized mirror maps have enhanced convergence rates and lower error floors. Our findings indicate that the choice of mirror map significantly impacts PMD’s effectiveness, an aspect not adequately reflected by the convergence guarantees reported in existing literature. Our research introduces several new directions for inquiry. From a theoretical perspective, understanding the impact of the mirror map on AMPO’s performance and on that of other PMD frameworks is an area for future exploration. On the practical side, investigating how specific environmental structures or temporal awareness Jackson et al. (2023) can inform the choice of a mirror map to improve performance represents another research focus.

References

Agarwal, A., Kakade, S. M., Lee, J. D., and Mahajan, G. On the theory of policy gradient methods: Optimality, approximation, and distribution shift. *Journal of Machine Learning Research*, 2021. 1, 5

Akiba, T., Sano, S., Yanase, T., Ohta, T., and Koyama, M. Optuna: A next-generation hyperparameter optimization framework, 2019. 8

Alfano, C., Yuan, R., and Rebeschini, P. A novel framework for policy mirror descent with general parametrization and linear convergence. *Advances in Neural Information Processing Systems*, 2023. 1, 2, 4, 5

Baxter, J. and Bartlett, P. L. Infinite-horizon policy-gradient estimation. *Journal of Artificial Intelligence Research*, 2001. 1

Berner, C., Brockman, G., Chan, B., Cheung, V., Debiak, P., Dennison, C., Farhi, D., Fischer, Q., Hashme, S., Hesse, C., et al. Dota 2 with large scale deep reinforcement learning. *arXiv preprint arXiv:1912.06680*, 2019. 1

Beyer, H.-G. Evolutionary algorithms in noisy environments: theoretical issues and guidelines for practice. *Computer Methods in Applied Mechanics and Engineering*, 2000. 2

Bhatnagar, S., Sutton, R. S., Ghavamzadeh, M., and Lee, M. Natural actor-critic algorithms. *Automatica*, 2009. 1

- Bregman, L. M. The relaxation method of finding the common point of convex sets and its application to the solution of problems in convex programming. *USSR Computational Mathematics and Mathematical Physics*, 1967. 3
- Bubeck, S. Convex optimization: Algorithms and complexity. *Foundations and Trends in Machine Learning*, 2015. 3
- Cen, S., Cheng, C., Chen, Y., Wei, Y., and Chi, Y. Fast global convergence of natural policy gradient methods with entropy regularization. *Operations Research*, 2021. 1
- Censor, Y. and Zenios, S. A. *Parallel Optimization: Theory, Algorithms, and Applications*. Oxford University Press, USA, 1997. 3
- Hansen, N. and Ostermeier, A. Completely derandomized self-adaptation in evolution strategies. *Evolutionary Computation*, 2001. 7
- Hu, Y., Ji, Z., and Telgarsky, M. Actor-critic is implicitly biased towards high entropy optimal policies. In *International Conference on Learning Representations*, 2022. 1, 5
- Jackson, M. T., Lu, C., Kirsch, L., Lange, R. T., Whiteson, S., and Foerster, J. N. Discovering temporally-aware reinforcement learning algorithms. In *Second Agent Learning in Open-Endedness Workshop*, 2023. 10
- Kakade, S. M. A natural policy gradient. *Advances in Neural Information Processing Systems*, 2002. 1
- Konda, V. and Tsitsiklis, J. Actor-critic algorithms. In *Advances in Neural Information Processing Systems*, 2000. 1
- Krichene, W., Krichene, S., and Bayen, A. Efficient bregman projections onto the simplex. In *IEEE Conference on Decision and Control*, 2015. 2, 5, 16
- Kuba, J. G., De Witt, C. A. S., and Foerster, J. Mirror learning: A unifying framework of policy optimisation. In *International Conference on Machine Learning*, 2022. 1
- Kullback, S. and Leibler, R. A. On Information and Sufficiency. *The Annals of Mathematical Statistics*, 1951. 1
- Laidlaw, C., Russell, S., and Dragan, A. Bridging rl theory and practice with the effective horizon. *Advances in Neural Information Processing Systems*, 2023. 9
- Lan, G. Policy mirror descent for reinforcement learning: Linear convergence, new sampling complexity, and generalized problem classes. *Mathematical programming*, 2022a. 1
- Lan, G. Policy optimization over general state and action spaces. *arXiv preprint arXiv:2211.16715*, 2022b. 2, 5
- Lange, R. T. evosax: Jax-based evolution strategies. *arXiv preprint arXiv:2212.04180*, 2022a. 8
- Lange, R. T. gymmax: A JAX-based reinforcement learning environment library, 2022b. URL <http://github.com/RobertTLange/gymmax>. 8
- Li, Y. and Lan, G. Policy mirror descent inherently explores action space. *arXiv preprint arXiv:2303.04386*, 2023. 2
- Liu, Q., Weisz, G., György, A., Jin, C., and Szepesvari, C. Optimistic natural policy gradient: a simple efficient policy optimization framework for online rl. *Advances in Neural Information Processing Systems*, 2023. 2
- Lu, C., Kuba, J., Letcher, A., Metz, L., Schroeder de Witt, C., and Foerster, J. Discovered policy optimisation. *Advances in Neural Information Processing Systems*, 2022. 2
- Lu, C., Willi, T., Letcher, A., and Foerster, J. N. Adversarial cheap talk. In *International Conference on Machine Learning*, 2023. 2
- Misra, D., Henaff, M., Krishnamurthy, A., and Langford, J. Kinematic state abstraction and provably efficient rich-observation reinforcement learning. In *International conference on machine learning*, 2020. 9

- Mnih, V., Badia, A. P., Mirza, M., Graves, A., Lillicrap, T., Harley, T., Silver, D., and Kavukcuoglu, K. Asynchronous methods for deep reinforcement learning. In *International Conference on Machine Learning*, 2016. 1
- Nemirovski, A. and Yudin, D. B. *Problem Complexity and Method Efficiency in Optimization*. Wiley Interscience, 1983. 1, 3
- Ouyang, L., Wu, J., Jiang, X., Almeida, D., Wainwright, C., Mishkin, P., Zhang, C., Agarwal, S., Slama, K., Ray, A., et al. Training language models to follow instructions with human feedback. *Advances in Neural Information Processing Systems*, 2022. 1
- Peters, J. and Schaal, S. Natural actor-critic. *Neurocomputing*, 2008. 1
- Real, E., Aggarwal, A., Huang, Y., and Le, Q. V. Regularized evolution for image classifier architecture search. *Proceedings of the AAAI Conference on Artificial Intelligence*, 2019. 2
- Ros, R. and Hansen, N. A simple modification in cma-es achieving linear time and space complexity. In *International conference on parallel problem solving from nature*, pp. 296–305. Springer, 2008. 7
- Salimans, T., Ho, J., Chen, X., Sidor, S., and Sutskever, I. Evolution strategies as a scalable alternative to reinforcement learning, 2017. 2
- Schulman, J., Levine, S., Abbeel, P., Jordan, M., and Moritz, P. Trust region policy optimization. In *International Conference on Machine Learning*, 2015. 1
- Schulman, J., Wolski, F., Dhariwal, P., Radford, A., and Klimov, O. Proximal policy optimization algorithms. *arXiv preprint arXiv:1707.06347*, 2017. 1
- Shalev-Shwartz, S., Shammah, S., and Shashua, A. Safe, multi-agent, reinforcement learning for autonomous driving. *arXiv preprint arXiv:1610.03295*, 2016. 1
- Such, F. P., Madhavan, V., Conti, E., Lehman, J., Stanley, K. O., and Clune, J. Deep neuroevolution: Genetic algorithms are a competitive alternative for training deep neural networks for reinforcement learning, 2018. 2
- Sutton, R. S., McAllester, D. A., Singh, S. P., and Mansour, Y. Policy gradient methods for reinforcement learning with function approximation. In *Advances in Neural Information Processing Systems*, 1999. 1
- Tomar, M., Shani, L., Efroni, Y., and Ghavamzadeh, M. Mirror descent policy optimization. In *International Conference on Learning Representations*, 2022. 1, 2, 5
- Vaswani, S., Bachem, O., Totaro, S., Müller, R., Garg, S., Geist, M., Machado, M. C., Castro, P. S., and Le Roux, N. A general class of surrogate functions for stable and efficient reinforcement learning. In *International Conference on Artificial Intelligence and Statistics*, 2022. 1, 2, 5
- Vaswani, S., Kazemi, A., Babanezhad, R., and Roux, N. L. Decision-aware actor-critic with function approximation and theoretical guarantees. *Advances in Neural Information Processing Systems*, 2023. 2, 5
- Williams, R. J. and Peng, J. Function optimization using connectionist reinforcement learning algorithms. *Connection Science*, 1991. 1
- Xiao, L. On the convergence rates of policy gradient methods. *Journal of Machine Learning Research*, 2022. 1, 2, 5
- Yuan, R., Du, S. S., Gower, R. M., Lazaric, A., and Xiao, L. Linear convergence of natural policy gradient methods with log-linear policies. In *International Conference on Learning Representations*, 2023. 2
- Zanette, A., Cheng, C.-A., and Agarwal, A. Cautiously optimistic policy optimization and exploration with linear function approximation. In *Conference on Learning Theory*, 2021. 2

A Further discussion on ω -potentials

A.1 Negative entropy

We show here that if $\phi(x) = e^{x-1}$, then the associated mirror map h_ϕ is the negative entropy. We have that

$$\int_0^1 \phi^{-1}(x)dx = \int_0^1 \log(x)dx = [x \log(x) - x]_0^1 = -1 \leq +\infty.$$

The mirror map h_ϕ becomes the negative entropy, up to a constant, as

$$h_\phi(\pi_s) = \sum_{a \in \mathcal{A}} \int_1^{\pi(a|s)} \log(x)dx = |\mathcal{A}| - 1 + \sum_{a \in \mathcal{A}} \pi(a|s) \log(\pi(a|s)).$$

A.2 Proofs for Section 3.1

Proposition A.1 (Proposition 3.3). *Let ϕ be an ω -potential and let (η, ϕ) and (η', ϕ') be equivalent for AMPO if they generate the same training path. We have that:*

- (shift-invariant) if $\phi'(x) := \phi(x + c)$, for $c \in \mathbb{R}$, then ϕ and ϕ' are equivalent for AMPO;
- (scale-invariant) if $(\eta', \phi'(x)) = (c\eta, \phi(x/c))$, for $c \in \mathbb{R}$, then (η, ϕ) and (η', ϕ') are equivalent for AMPO.

Proof. (Shift-invariant) If $\phi'(x) := \phi(x + c)$, then the policy induced by AMPO using ϕ' can be expressed as

$$\begin{aligned} \pi^{t+1}(a|s) &= \sigma(\phi'(\eta f^{t+1}(s, a) + (\lambda')_s^{t+1})) \\ &= \sigma(\phi(\eta f^{t+1}(s, a) + c + (\lambda')_s^{t+1})) \\ &= \sigma(\phi(\eta f^{t+1}(s, a) + \lambda_s^{t+1})). \end{aligned}$$

Since λ_s^{t+1} and $(\lambda')_s^{t+1}$ are normalization constants, the constant c will not affect the policy. Similarly, the minimization problem in step 1) of Algorithm 1 becomes

$$\begin{aligned} \theta^{t+1} &\in \operatorname{argmin}_{\theta \in \Theta} \|f^\theta - Q^t - \eta^{-1} \max(\eta f^t, (\phi')^{-1}(0) - (\lambda')_s^t)\|_{L_2(v^t)}^2 \\ &= \operatorname{argmin}_{\theta \in \Theta} \|f^\theta - Q^t - \eta^{-1} \max(\eta f^t, \phi^{-1}(0) - \lambda_s^t)\|_{L_2(v^t)}^2. \end{aligned}$$

(Scale-invariant) If $(\eta', \phi'(x)) = (c\eta, \phi(x/c))$, then the policy induced by AMPO using ϕ' can be expressed as

$$\begin{aligned} \pi^{t+1}(a|s) &= \sigma(\phi'(\eta' f^{t+1}(s, a) + (\lambda')_s^{t+1})) \\ &= \sigma(\phi(\eta f^{t+1}(s, a) + c^{-1}(\lambda')_s^{t+1})) \\ &= \sigma(\phi(\eta f^{t+1}(s, a) + \lambda_s^{t+1})). \end{aligned}$$

Similarly, the minimization problem in step 1) of Algorithm 1 becomes

$$\begin{aligned} \theta^{t+1} &\in \operatorname{argmin}_{\theta \in \Theta} \|f^\theta - Q^t - (\eta')^{-1} \max(\eta' f^t, (\phi')^{-1}(0) - (\lambda')_s^t)\|_{L_2(v^t)}^2 \\ &= \operatorname{argmin}_{\theta \in \Theta} \|f^\theta - Q^t - \eta^{-1} \max(\eta f^t, \phi^{-1}(0) - \lambda_s^t)\|_{L_2(v^t)}^2. \end{aligned}$$

□

We also give a proof for the statements regarding the derivative of the policy w.r.t. a change in score difference. Assume that $\mathcal{A} = \{a_1, a_2\}$ and, for an arbitrary state s and iteration t , let $b, c \in \mathbb{R}$ such that $\eta f^{t+1}(s, a_1) = \eta f^t(s, a_1) + b + c$ and $\eta f^{t+1}(s, a_2) = \eta f^t(s, a_2) + b$. In this setting, where the score difference

between the two actions has increased (or diminished) by a factor c , we have that the derivative of the updated policy w.r.t. c is

$$\begin{aligned}\frac{d\pi(a_1|s)}{dc} &= \frac{\phi'(x_1)\phi'(x_2)}{\phi'(x_1) + \phi'(x_2)}, \\ \frac{d\pi(a_2|s)}{dc} &= -\frac{\phi'(x_1)\phi'(x_2)}{\phi'(x_1) + \phi'(x_2)},\end{aligned}$$

where $x_i = \eta f^{t+1}(s, a_i) + \lambda_s^{t+1}$.

Proof. Since $\sum_{i=1}^2 \phi(x_i) = 1$ regardless of the value of c , we have that $\sum_{i=1}^2 \frac{d\phi(x_i)}{dc} = 0$. Given

$$\sum_{i=1}^2 \frac{d\phi(x_i)}{dc} = \sum_{i=1}^2 \phi'(x_i) \frac{dx_i}{dc} = \sum_{i=1}^2 \phi'(x_i) \left(\frac{dx_i}{dc} - \frac{dx_j}{dc} + \frac{dx_j}{dc} \right),$$

we have that

$$\sum_{i=1}^2 \phi'(x_i) \left(\frac{dx_j}{dc} - \frac{dx_i}{dc} \right) = \sum_{i=1}^n \phi'(x_i) \frac{dx_j}{dc},$$

and

$$\begin{aligned}\frac{dx_j}{dc} &= \frac{\sum_{i=1}^2 \phi'(x_i) \left(\frac{dx_j}{dc} - \frac{dx_i}{dc} \right)}{\sum_{i=1}^2 \phi'(x_i)}, \\ \frac{d}{dc}(\phi(x_j)) &= \phi'(x_j) \frac{\sum_{i=1}^2 \phi'(x_i) \left(\frac{dx_j}{dc} - \frac{dx_i}{dc} \right)}{\sum_{i=1}^2 \phi'(x_i)}.\end{aligned}$$

Therefore, we can conclude that

$$\begin{aligned}\frac{d}{dc}(\phi(x_1)) &= \frac{\phi'(x_1)\phi'(x_2)}{\phi'(x_1) + \phi'(x_2)}, \\ \frac{d}{dc}(\phi(x_2)) &= -\frac{\phi'(x_1)\phi'(x_2)}{\phi'(x_1) + \phi'(x_2)}.\end{aligned}$$

□

A.3 Exact ϕ used in Figure 1

Here we provide the exact expressions for the functions we displayed in Figure 1. Note that all these functions are shift invariant, and we simply include shift constants to make the different functions line up for visual clarity. Furthermore, the other constants have no particular meaning, and were selected simply to show a variety of behaviours. We include the exact functions we used for the sake of completeness:

$$\begin{aligned}exp(x) &= \min(e^{x-0.5}, 1), \\ sigmoid(x) &= (1 + e^{-2.1x})^{-1}, \\ double_sigmoid(x) &= 0.5(1 + e^{-4.2x+3})^{-1} \\ &\quad + 0.5(1 + e^{-8.4x-8})^{-1}, \\ many_sigmoids(x) &= 0.2 \sum_{i=1}^5 \left(1 + e^{-10(2.1x-w_i)} \right)^{-1},\end{aligned}$$

where $w = [-3, -1.5, 0, 1.5, 3]$.

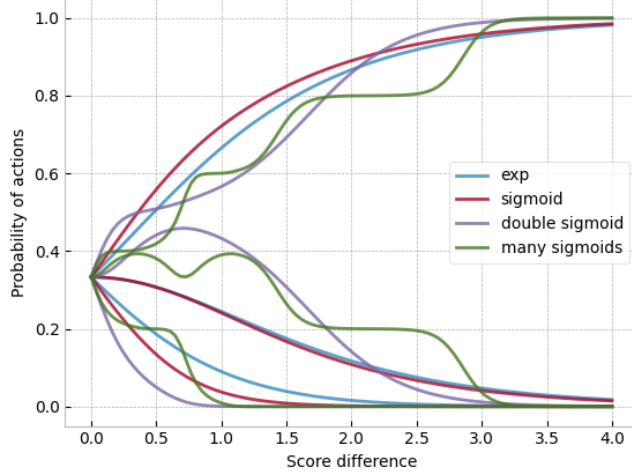


Figure 4: Showing action distribution across different mirror maps when having multiple, 3, different actions. The scores are equal to $[0, 1, 2] \times \text{Score difference}$

A.4 Multiple-action policies

We show in Figure 4 the induced distributions for a policy with three actions and for different scores, for the same ω -potentials as in Figure 1. We also give an extension on the statement regarding the gradient of the policy w.r.t. a change in scores. Assume that $\mathcal{A} = \{a_i\}_{i=1,\dots,n}$ and, for an arbitrary state s and iteration t , let $c \in \mathbb{R}^n$ such that $\eta f_s^{t+1} = \eta f_s^t + c$. In this setting, we have that the derivative of the updated policy w.r.t. c is

$$\nabla_c \pi_s = \text{diag}(\phi'(x)) - \frac{\phi'(x)\phi'(x)^\top}{\mathbf{1}^\top \phi'(x)},$$

where $x_i = \eta f_s^{t+1}(s, a_i) + \lambda_s^{t+1}$, ϕ' is applied element-wise, $\mathbf{1}$ is a vector with all entries equal to 1, and, for vector $w \in \mathbb{R}^n$, $\text{diag}(w)$ is the square diagonal $n \times n$ matrix with $\text{diag}(w)_{i,i} = w_i$.

Proof. We have that

$$\begin{aligned} \nabla_c \pi_s &= \text{diag}(\phi'(x)) \nabla_c x \\ &= \text{diag}(\phi'(x)) (I + \nabla_c \lambda_s^{t+1} \mathbf{1}) \\ &= \text{diag}(\phi'(x)) + \phi'(x) (\nabla_c \lambda_s^{t+1})^\top. \end{aligned} \tag{10}$$

Since $\mathbf{1}^\top \pi_s = 1$ regardless of c , we also have that $\mathbf{1}^\top \nabla_c \pi_s = \mathbf{0}$, where $\mathbf{1}$ and $\mathbf{0}$ are vectors with entries all equal to 1 and 0, respectively. Therefore, we have that

$$\mathbf{1}^\top \nabla_c \pi_s = \mathbf{1}^\top \text{diag}(\phi'(x)) + \mathbf{1}^\top \phi'(x) \nabla_c \lambda_s^{t+1} = 0$$

and

$$\nabla_c \lambda_s^{t+1} = -\frac{\phi'(x)}{\mathbf{1}^\top \phi'(x)},$$

which concludes the proof by replacing in (10). \square

A.5 Parametric ϕ

We show here that the parametric class of ω -potentials we introduce in Section 4 results in a well defined algorithm when used for AMPO, even if it breaks some of the constraints in Theorem 3.2. In particular, ω -potentials within Φ are not C^1 -diffeomorphisms and are only non-decreasing. We can afford not meeting the first constraint

as the proof for Theorem 1 by Krichene et al. (2015), which establishes the computational complexity for a Bregman projection using ω -potentials, only requires Lipschitz-continuity. As to the second constraint, we build an augmented class Φ' that contains increasing ω -potentials and show that it results in the same updates for AMPO as Φ .

Let Δ_n be the n -dimensional probability simplex. We define the parameterized class $\Phi' = \{\phi'_\psi : \mathbb{R} \rightarrow [0, 1], \psi \in \Delta_n\}$, with

$$\phi'_\psi(x) = \begin{cases} e^x - 1 & \text{if } x \leq 0, \\ \frac{x}{\psi_1 n} & \text{if } 0 < x \leq \psi_1, \\ \frac{j}{n} + \frac{x - \sum_{i=1}^j \psi_i}{n\psi_{j+1}} & \text{if } \sum_{i=1}^j \psi_i < x \leq \sum_{i=1}^{j+1} \psi_i, \\ x & \text{if } x > 1, \end{cases}$$

where $1 \leq j \leq n-1$. The functions within Φ' are increasing and continuous. We start by showing that $\phi'_\psi \in \Phi'$ and $\phi_\psi \in \Phi$ are equivalent for the Bregman projection step, for the same parameters ψ . At each iteration t , we have that

$$\begin{aligned} \pi^{t+1}(a | s) &= \sigma(\phi'(\eta f^{t+1}(s, a) + (\lambda')_s^{t+1})) \\ &= \sigma(\phi(\eta f^{t+1}(s, a) + (\lambda')_s^{t+1})) \\ &= \sigma(\phi(\eta f^{t+1}(s, a) + \lambda_s^{t+1})). \end{aligned}$$

This due to the following two facts. For $x \leq 0$, $\sigma(\phi'(x))$ and $\sigma(\phi(x))$ are the same function. Also, $\sigma(\phi'(\eta f^{t+1}(s, a) + (\lambda')_s^{t+1}))$ has to be less or equal to 1, as a result of the projection, meaning that $\eta f^{t+1}(s, a) + (\lambda')_s^{t+1} \leq 1$, where $\sigma(\phi'(\cdot))$ and $\sigma(\phi(\cdot))$ are equivalent.

Since ϕ and ϕ' induce the same projection, share that same normalization constant, and have the same value at 0, they also induce the same expression for step 1) in Algorithm 1.

B Training details

B.1 Hyper-parameters for AMPO

We give the hyper-parameters we use for training in Table 1.

Table 1: Hyper-parameter settings for different environments

Parameter	Acrobot-v1	CartPole-v1	Asterix	Breakout	Freeway	SpaceInvaders
ACTIVATION	tanh	tanh	tanh	tanh	tanh	tanh
ANNEAL LR	True	True	True	True	True	True
VALUE LOSS CLIP	0.2	0.2	0.2	0.2	0.2	0.2
GAE LAMBDA	0.95	0.95	0.95	0.95	0.95	0.95
GAMMA	0.99	0.999	0.999	0.99	0.99	0.999
LR	1e-3	8.95e-3	5.0e-4	4.9e-4	4.9e-4	5.0e-4
ETA	1.0	1.9	1.0	0.9	0.9	1.0
MAX GRAD NORM	0.5	1.0	5.0	2.4	2.4	3.5
NUM ENVIS	10	16	32	64	64	64
NUM MINIBATCHES	4	4	2	16	16	16
NUM STEPS	128	32	128	32	32	128
TOTAL TIMESTEPS	5e5	5e5	1e7	1e7	1e7	1e7
UPDATE EPOCHS	10	4	16	8	8	8
ACTOR-VALUE LOSS RATIO	0.5	0.5	0.5	0.5	0.5	0.5

B.2 Optimizing ϕ details

When we perform optimization, suppose we parameterise ϕ with N segments. Then, we optimize over $N + 1$ parameters, η^L and $\psi_i^L, i \in [1 \dots N]$, where $\eta = |\eta^L|$ and ψ is given by:

$$\psi_i = \frac{|\psi_i^L|}{\sum_{j=1}^N |\psi_j^L|}.$$

This ensures that our resulting values are positive and valid. Note this does add a degree of redundancy, multiplying ψ^L by a constant leaves ψ unchanged. However, this is reasonable trade-off for a more stable learning process.

B.3 Transferability of learned mirror maps

Here we show our raw transfer results in Table 2 and 3. Note that the Table 3 is a row-normalised version of Table 2, that is for each row (testing environment) a linear transformation is applied to set the mean to 0 and standard deviation to 1.

Testing \ Training	Acrobot-v1	CartPole-v1	Asterix	Breakout	Freeway	SpaceInvaders
Acrobot-v1	-161.99	-461.95	-469.04	-188.1	-449.06	-439.54
CartPole-v1	378.36	438.17	436.61	107.14	431.26	422.64
Asterix	3.4	14.31	14.43	1.9	15.55	4.19
Breakout	21.27	13.53	14.3	37.84	13.02	18.31
Freeway	0.13	51.35	50.66	1.67	51.29	0.23
SpaceInvaders	119.43	96.65	98.93	18.63	97.33	122.98

Table 2: Transfer Matrix, raw rewards.

Testing \ Training	Acrobot-v1	CartPole-v1	Asterix	Breakout	Freeway	SpaceInvaders
Acrobot-v1	1.51	-0.76	-0.81	1.31	-0.66	-0.59
CartPole-v1	0.08	0.58	0.57	-2.2	0.52	0.45
Asterix	-0.95	0.91	0.93	-1.21	1.13	-0.81
Breakout	0.18	-0.72	-0.63	2.1	-0.78	-0.16
Freeway	-1.02	1.01	0.98	-0.96	1.01	-1.02
SpaceInvaders	0.78	0.12	0.19	-2.13	0.14	0.89

Table 3: Transfer Matrix, normalised per-environment scores.